Electronic Supplementary Material (ESI) for Analyst.

Supporting Information

Aggregation-induced Emission Enhancement of Gold Nanoclusters in Metal–organic Frameworks for Highly Sensitive Fluorescent Detection of Bilirubin

Mengfan Xia[a,b], Yucun Sui[a,b], Ying Guo[a,b], Yaodong Zhang[a,b,*]

[a]Key Laboratory of Applied Surface and Colloid Chemistry of Ministry of Education, [b]Key Laboratory of Analytical Chemistry for Life Science of Shaanxi Province, School of Chemistry and Chemical Engineering, Shaanxi Normal University, Xi'an 710062, PR China.

* Corresponding author.

E-mail: ydzhang@snnu.edu.cn; Fax: +86-29-81530727; Tel: +86-29-81530726

Table of Contents

Section S1. Characterization of ZIF-8 and AuNCs@ZIF-8

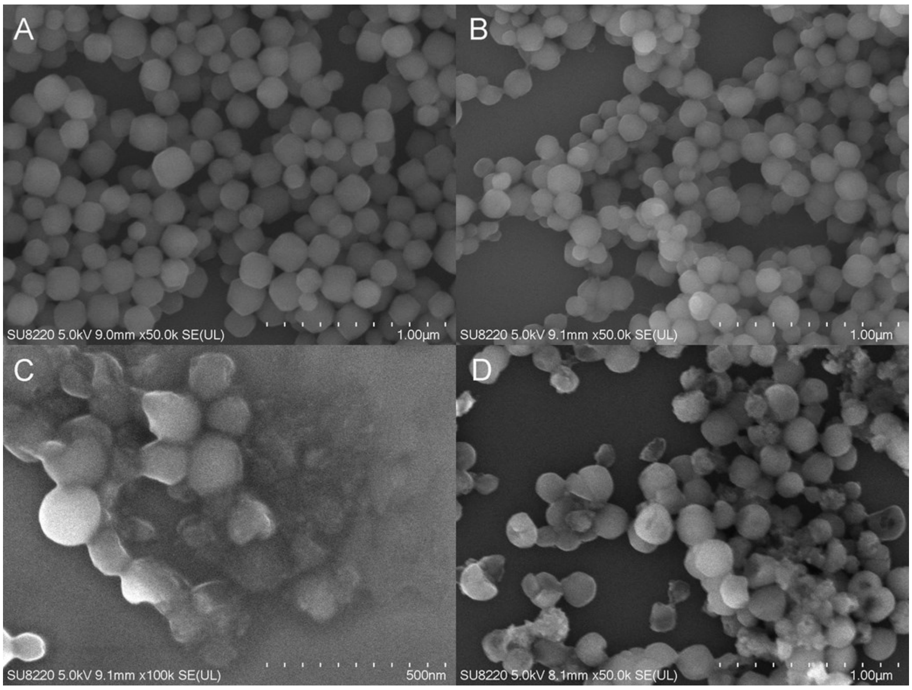

Figure S1.SEM images of ZIF-8(A) ,AuNCs@ZIF-8(B) and AuNCs@ZIF-8 after adding BR(C,D)

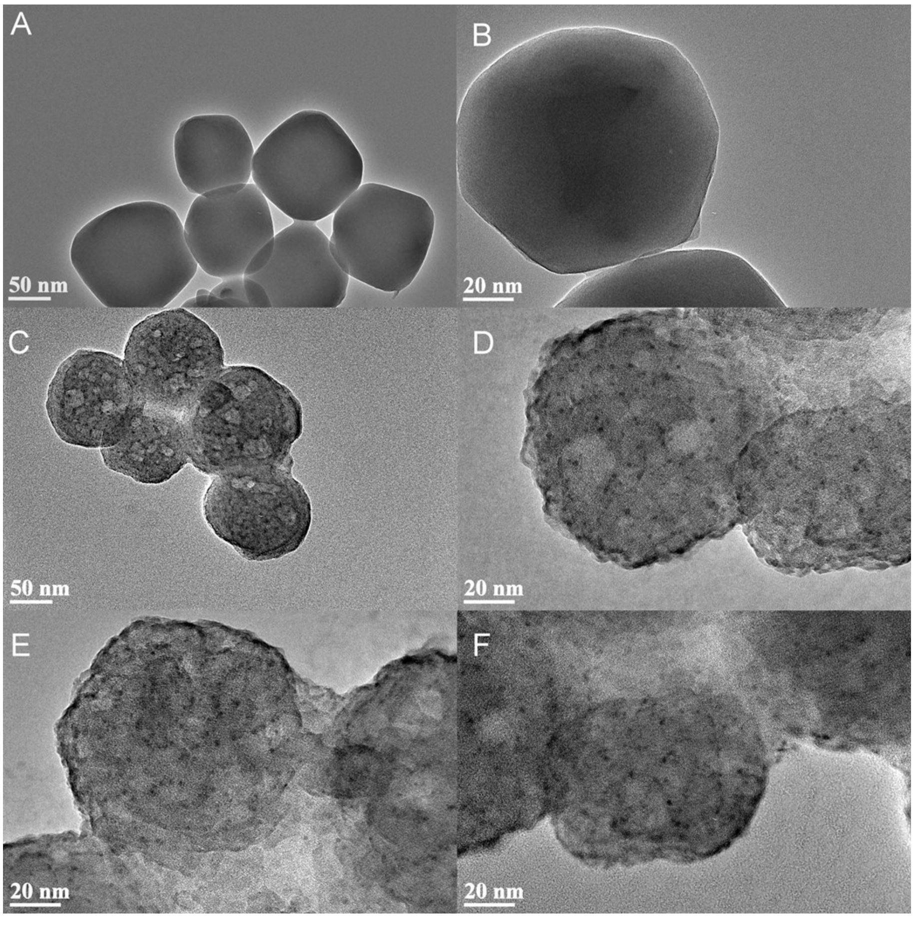

Figure S2. TEM images of ZIF-8(A,B) and AuNCs@ZIF-8(C,D,E,F)

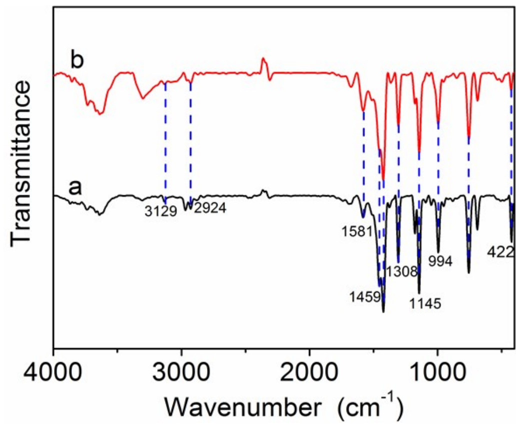

Figure S3. FTIR spectra for ZIF-8(a) and AuNCs@ZIF-8(b) (The peak at 422 cm^{-1} is attributed to the Zn-N stretching vibration. The bands in the spectral region of 500–1350 cm^{-1} (994 cm^{-1}, 1145 cm^{-1} and 1308 cm^{-1})are assigned as the plane bending and stretching of imidazole ring, respectively. The C=N stretch mode which is expected at 1459 cm^{-1} and 1581 cm^{-1}. The absorption peaks at 2924 cm^{-1} and 3129 cm^{-1} are due to the N-H and C-H stretching vibrations, respectively.[1, 2])

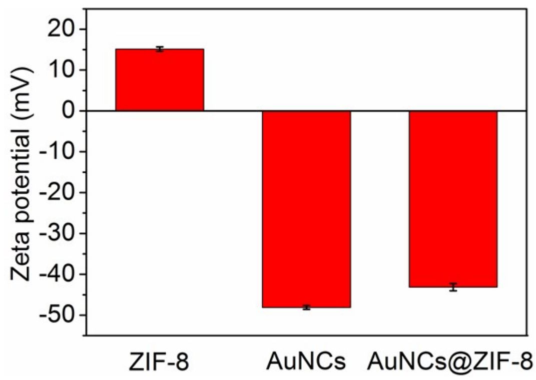

Figure S4. Zeta potential for ZIF-8, AuNCs and AuNCs@ZIF-8

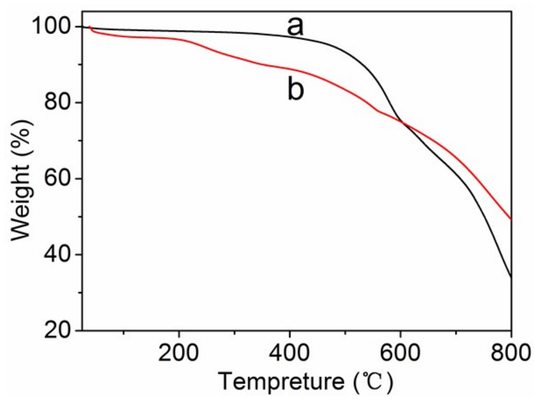

Figure S5. TGA curve of ZIF-8(a) and AuNCs@ZIF-8(b)

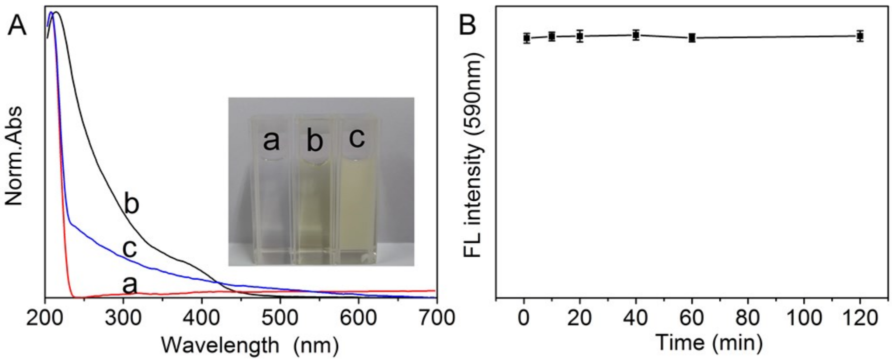

Figure S6. (A) UV–vis absorption spectra of ZIF-8(a), AuNCs (b), and AuNCs @ZIF-8 (c). The inset shows the photographs of ZIF-8(a), AuNCs (b), and AuNCs@ZIF-8 (c) under daylight. (B) Fluorescence intensity variation in AuNCs@ZIF-8 for 120 min.

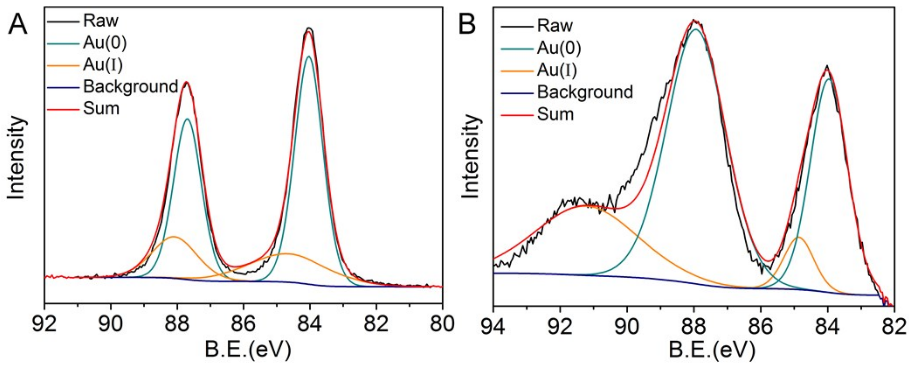

Figure S7. XPS spectrum of Au NCs (A) and AuNCs@ZIF-8 (B)

Section S2. Response time of AuNCs@ZIF-8 to BR

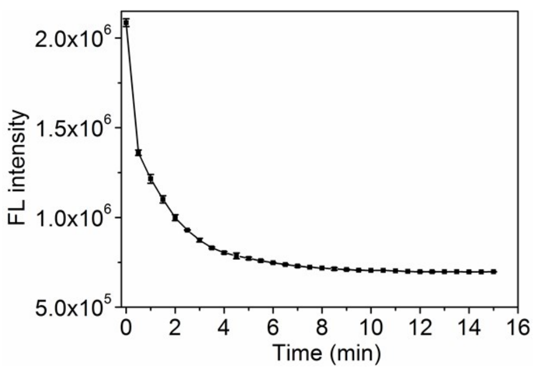

Figure S8. Time-dependent fluorescence emission intensity of AuNCs@ZIF-8 upon the addition of bilirubin (6 μM)

Section S3. Possible mechanism of AuNCs@ZIF-8 for sensing BR

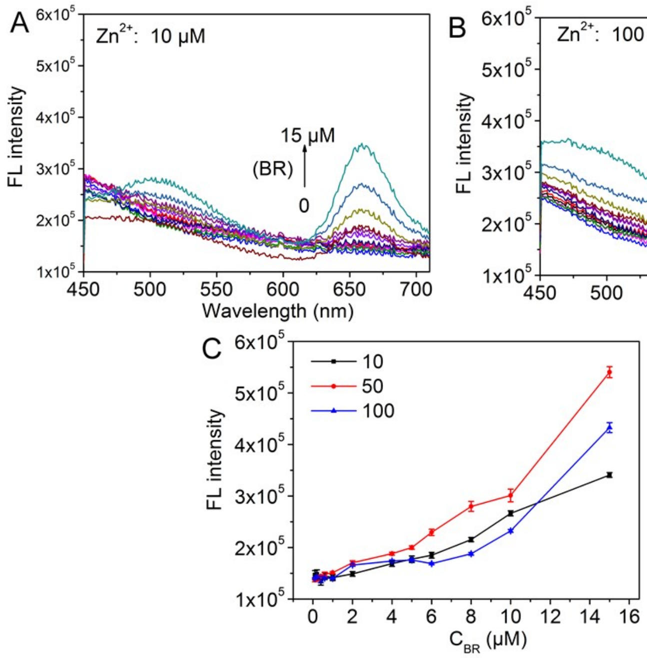

Figure S9. Fluorescence emission spectra of Zn^{2+} (10 μM, A) or Zn^{2+} (100 μM, B) with different concentrations of BR. (C) Fluorescence emission intensity (660 nm) of different concentrations of Zn^{2+} with different concentrations of BR.

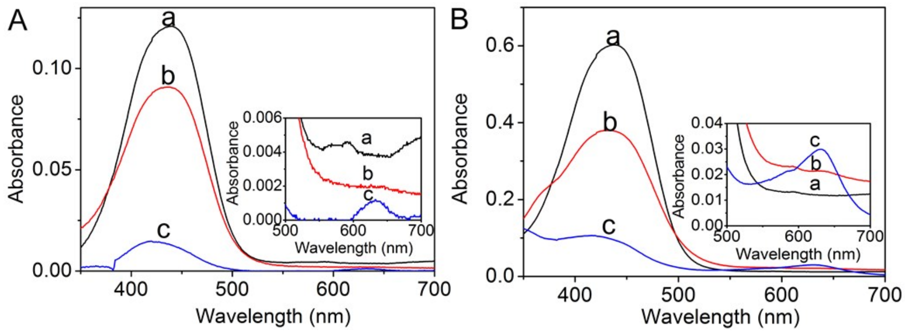

Figure S10. (A) UV–vis absorption spectra of BR (2 μM, a) with Zn^{2+} (50 μM, b) or AuNCs@ZIF-8 (0.06 mg/mL, c) after centrifugation (inset: magnified view between 500–700 nm). (B) UV–vis absorption spectra of BR (10 μM, a) with Zn^{2+}(50 μM, b) or AuNCs@ZIF-8 (0.06 mg/mL, c) after centrifugation (inset: magnified view between 500–700 nm)

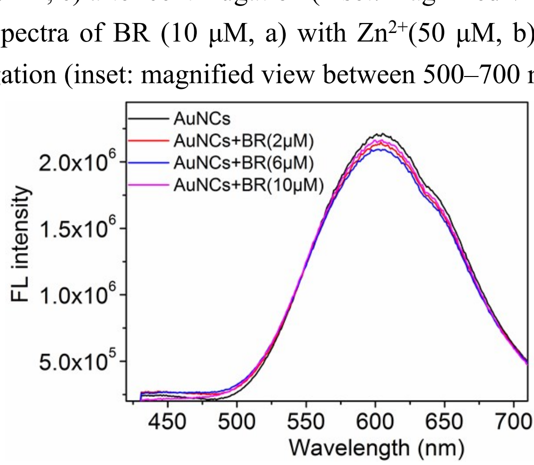

Figure S11. Emission spectra of Au NCs containing different concentrations of BR.

Section S4. Comparison of the performance of methods for detection of BR

Table S1. Comparison of the performance of methods for detection of BR

Materials	Principle	Linear Range	LOD	Reference
HAS-AuNCs	Interaction between BR and HSA	1-50 μM	0.248 μM	3
HSA–CuNCs	Binding attraction between BR and HAS-CuNCs	1.25-7.50 μM 5.00-28.75 μM	0.035μM 0.145μM	4
BSA-Cu Nanoclusters	Fluorescence regain by the addition of BR to Fe^{3+} + BSA-CuNCs	0.1 pM-0.1μM	6.62 nM	5
Mn:ZnS QDs	PET*	10.99-63.84 μM	1.8 μM	6
MoS_2 QDs	FRET* and IIF*	0.5-10 μM	2.1 nM	7
UiO-66$(COOH)_2$:Eu	FRET	0-15 μM	0.45μM	8
Eu-MOFs	PET and IIF	0-56.6 μM	1.75 μM	9
$Eu(tta)_3$	Special σ-hole bonding between Htta and BR	0-50 μM	0.068 μM	10
AuNCs@ZIF-8	AIEE*	0.1-5 μM	0.07 μM	This work

(PET*: Photoinduced Electron Transfer. FRET*: Fluorescent Resonant Energy Transfer. IIF*: Inner Filter Effect. AIEE*:Aggregation-induced Emission Enhancement)

References

1 Y. Hu, H. Kazemian, S. Rohani, Y. Huang and Y. Song, *Chem. Commun.*, 2011, **47**, 12694-12696.

2 S. Chao, X. Li, Y. Li, Y. Wang and C. Wang, *J. Colloid Interface Sci.*, 2019, **552**, 506-516.

3 M. Santhosh, S.R. Chinnadayyala, A. Kakoti, P. Goswami, *Biosens. Bioelectron*. 2014, **59**, 370-376.

4 R. Rajamanikandan, M. Ilanchelian, *Mater. Sci. Eng. C* , 2019, **98**, 1064-1072.

5 M. Jayasree, R.S. Aparna, R.R. Anjana, J.S. Anjali Devi, N. John, K. Abha, A. Manikandan, S. George, *Anal. Chim. Acta*, 2018, **1031**, 152-160.

6 K. Abha, J. Nebu, J.S. Anjali Devi, R.S. Aparna, R.R. Anjana, A.O. Aswathy, S. George, *Sensor. Actuator. B Chem.* , 2019, **282**, 300-308.

7 K. Shanmugaraj, S.A. John, *Spectrochim. Acta, Part A* ,2019, **215**, 290-296.

8 C. Xia, Y. Xu, M.-M. Cao, Y.-P. Liu, J.-F. Xia, D.-Y. Jiang, G.-H. Zhou, R.-J. Xie, D.-F. Zhang, H.-L. Li, *Talanta*,2020, **212** , 120795.

9 P. Xu, H.-W. Yang, J.-L. Shi, B. Ding, X.-J. Zhao, E.-C. Yang, *RSC Adv.*,2019, **9**,37584-37593.

10 W. Yang, J. Xia, G. Zhou, D. Jiang, Q. Li, S. Wang, X. Zheng, X. Li, Y. Shen, X. Li, *Anal. Bioanal. Chem.*,2018, **410**, 6459-6468.